

Control of HIF-1 α Expression by eIF2 α Phosphorylation–Mediated Translational Repression

Keyi Zhu,^{1,2} WaiKin Chan,³ John Heymach,^{1,4} Miles Wilkinson,³ and David J. McConkey^{1,2}

Departments of ¹Cancer Biology, ²Urology, ³Biochemistry and Molecular Biology and ⁴Thoracic/Head and Neck Oncology, The University of Texas M. D. Anderson Cancer Center, Houston, Texas

Abstract

Hypoxia inducible factor 1 α (HIF-1 α) plays a central role in regulating tumor angiogenesis via its effects on vascular endothelial growth factor (VEGF) transcription, and its expression is regulated through proteasome-mediated degradation. Paradoxically, previous studies have shown that proteasome inhibitors (PI) block tumor angiogenesis by reducing VEGF expression, but the mechanisms have not been identified. Here, we report that PIs down-regulated HIF-1 α protein levels and blocked HIF-1 α transcriptional activity in human prostate cancer cells. PIs induced phosphorylation of the translation initiation factor 2 α (eIF2 α), which caused general translational repression to inhibit HIF-1 α expression. Furthermore, PIs induced HIF-1 α accumulation in LNCaP-Pro5 cells depleted of eIF2 α via siRNA transfection and in MEFs expressing a phosphorylation-deficient mutant form of eIF2 α . Finally, PIs failed to induce eIF2 α phosphorylation or translational attenuation in DU145 or 253JB-V cells, and, in these cells, PIs promoted HIF-1 α accumulation. Our data established that PIs down-regulated HIF-1 α expression in cells that display activation of the unfolded protein response by stimulating phosphorylation of eIF2 α and inhibiting HIF-1 α translation. [Cancer Res 2009;69(5):1836–43]

Introduction

The 26S proteasome is a large, multicatalytic enzyme that functions as a major route of intracellular protein degradation (1–3). Bortezomib (PS-341/Velcade; Millennium Pharmaceuticals, Inc.) is a peptide boronate inhibitor of the chymotryptic activity of the proteasome that received Food and Drug Administration approval for the treatment of multiple myeloma and mantle cell lymphoma (1, 2, 4). Its clinical success has prompted other companies to develop chemically distinct proteasome inhibitors (PI) that might be even more active. One such compound is NPI-0052 (*salinosporamide A*; Nereus Pharmaceuticals), a structural analogue of the PI lactacystin that is currently being evaluated in phase I clinical trials. NPI-0052 is orally bioactive, irreversible, and has broader proteasome inhibitory activity than bortezomib (5, 6).

Analyses of the direct cytotoxic effects of PIs in tumor cells have identified a number of different biochemical mechanisms, including inhibition of prosurvival transcription factor nuclear factor κ B (NF κ B), accumulation of proapoptotic proteins, such as p53, Bax,

and NOXA, and induction of endoplasmic reticular (ER) stress (2, 3, 7, 8). PIs also suppress angiogenesis by down-regulating vascular endothelial growth factor (VEGF) expression (5, 9). Tumor VEGF expression is controlled in large part by the transcription factor hypoxia inducible factor 1 (HIF-1; refs. 10, 11), a heterodimer composed of an O₂ sensitive α subunit (HIF-1 α) and a constitutively expressed β subunit (HIF-1 β /ARNT; ref. 10). Under normoxic conditions, HIF-1 α is hydroxylated at two proline residues (P402 and P564) by prolyl hydroxylase-domain proteins and is subsequently recognized by Von Hippel-Lindau (VHL), a component of an E3 ubiquitin-protein ligase that targets HIF-1 α for degradation by the proteasome (10). Under hypoxic conditions, HIF-1 α is not hydroxylated and it accumulates. Loss of VHL expression is a common feature of renal cell carcinoma that results in overexpression of VEGF and increased angiogenesis (12). Overexpression of HIF-1 α has been observed in many other solid tumors, including prostate, breast, lung, and head and neck cancers, and chemical inhibitors of HIF-1 α are being developed for cancer therapy (10, 13–15).

It seemed paradoxical to us that HIF-1 α expression is controlled primarily by the proteasome, yet PIs down-regulate VEGF expression. We therefore initiated the present study to characterize the effects of PIs on HIF-1 α function. Here, we report that bortezomib and NPI-0052 selectively blocked the expression and activity of HIF-1 α in a subset of human prostate cancer cells. Analyses of the biochemical mechanisms implicated processes observed during ER stress, including phosphorylation of eIF2 α leading to inhibition of HIF-1 α translation. Similar effects were observed in cells exposed to other stimuli known to induce eIF2 α phosphorylation, indicating that the response may have broader biological significance.

Materials and Methods

Cell lines and culture. Human LNCaP-Pro5 prostate cancer cells and 253JB-V bladder cancer cells were provided by Dr. Curtis Pettaway and Dr. Colin Dinney, respectively (Department of Urology, University of Texas M. D. Anderson Cancer Center, TX). Human PC3 and DU145 prostate cancer cells were obtained from American Type Culture Collection. eIF2 α ^{51SS} wild-type and eIF2 α ^{51AA} knock-in mutant mouse embryonic fibroblast cells (MEF) were kindly provided by Dr. David Ron (New York University School of Medicine, New York, NY). The prostate cancer cells were grown in RPMI 1640 (Life Technologies, Inc.) supplemented with 10% fetal bovine serum (FBS; Life Technologies), 1% vitamins (Life Technologies), sodium pyruvate (Bio Whittaker), L-glutamine (Bio Whittaker), penicillin/streptomycin solution (Bio Whittaker), and nonessential amino acids (Life Technologies) under conditions of 5% CO₂ at 37°C in an incubator. 253JB-V cells were cultured in MEM medium containing the same supplements. The MEFs were grown in dMEM supplemented with 10% FBS, 1% penicillin/streptomycin solution, L-glutamine, nonessential amino acids, 55 mmol/L β -mercaptoethanol. Leucine-free medium was purchased from MP Biomedicals for measuring protein synthesis. For hypoxic exposure, cells were placed in a NAPCO Water-Jacketed CO₂ incubator (Thermo Fisher

Note: Supplementary data for this article are available at *Cancer Research* Online (<http://cancerres.aacrjournals.org/>).

Requests for reprints: David McConkey, Departments of Urology and Cancer Biology, University of Texas M. D. Anderson Cancer Center, 1515 Holcombe Boulevard, Houston, TX 77030. Phone: 713-792-8591; Fax: 713-792-8747; E-mail: dmcconke@mdanderson.org.

©2009 American Association for Cancer Research.
doi:10.1158/0008-5472.CAN-08-4103

Scientific, Inc.) flushed with 0.2% oxygen, 5% CO₂, and 95% nitrogen. Hypoxia was also mimicked by incubating cells with cobalt chloride (CoCl₂) in a regular atmosphere.

Reagents, antibodies, and plasmids. The PI bortezomib and the I κ B kinase (IKK)/NF κ B inhibitor PS-1145 were provided by Millenium Pharmaceuticals. The PI NPI-0052 was provided by Nereus Pharmaceuticals. Cycloheximide (CHX), thapsigargin, tunicamycin, heparin, and CoCl₂ were purchased from Sigma Co. Antibodies were obtained from the following commercial sources: human HIF-1 α and p21^{WAF1} (BD Biosciences Transduction Laboratories); HIF-2 α , HIF-1 β and mouse HIF-1 α (Novus Biologicals, Inc.); phosphorylated eIF2 α (Ser52) and total eIF2 α (Invitrogen Biosource); phosphorylated eIF2 α (Ser51) (Cell Signaling Technology, Inc.);

phosphorylated PERK(Thr851), P300, and Ref-1 (Santa Cruz Biotechnology); and actin (Sigma Chemical Co.). Horseradish peroxidase-conjugated secondary antibodies were obtained from Amersham Pharmacia Biotech (Piscataway). Hypoxia response element (HRE)-driven firefly luciferase plasmid was purchased from Panomics, Inc.

Immunoblotting. Total cell lysates were prepared using a 1% Triton X-100 buffer as described previously (16). Densitometric quantification of proteins levels was performed using ImageJ software (NIH).

Quantification of VEGF by ELISAs. LNCaP-Pro5 cells (5×10^4 cells per well) were plated in 24-well plates and were incubated with indicated chemicals for 24 h under normoxic or hypoxic conditions (0.2% O₂). Medium were then collected and VEGF levels were determined using

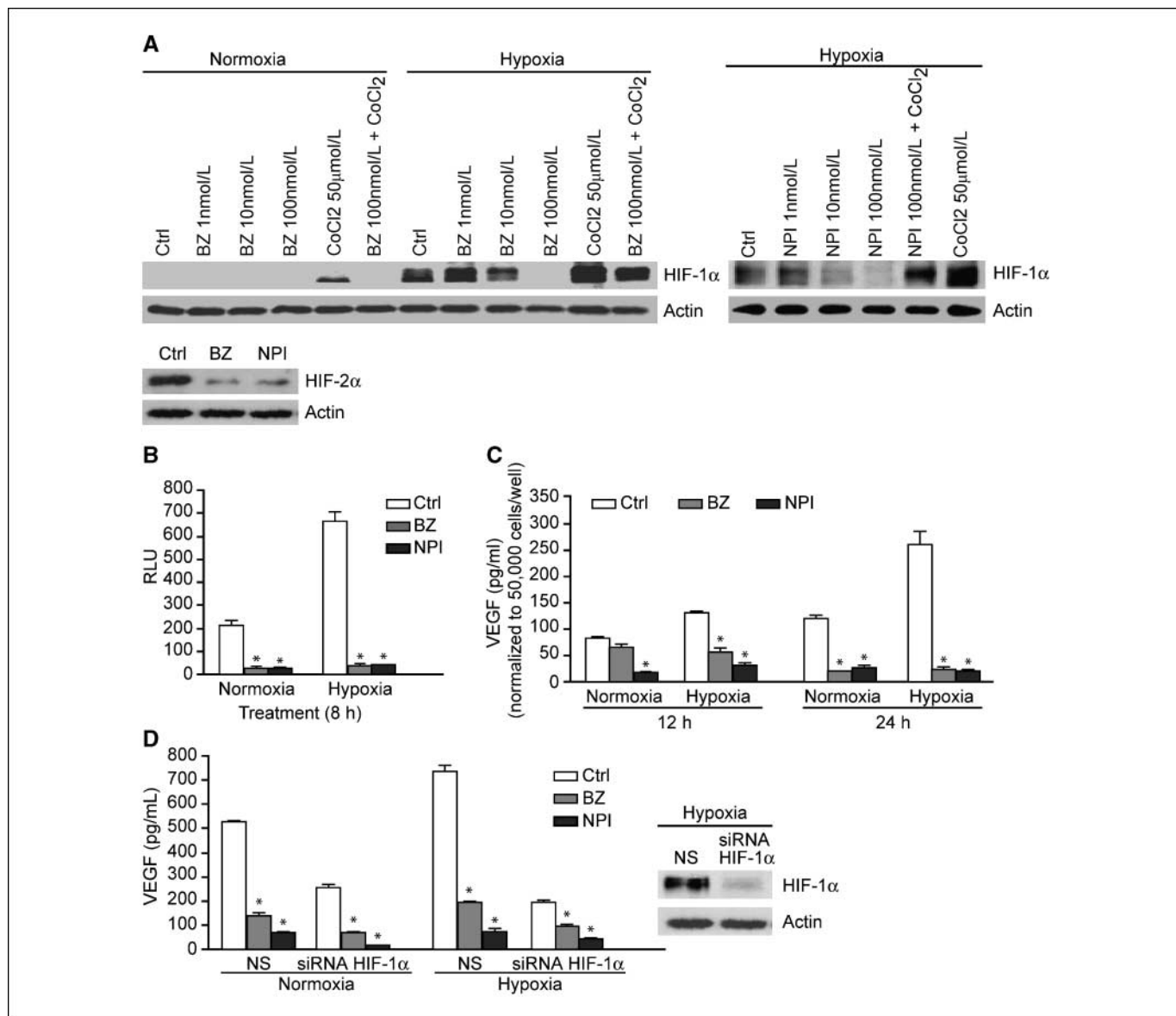


Figure 1. Effects of PIs on HIF-1 α , HIF-2 α , and VEGF expression. **A**, PIs down-regulate HIF-1 α and HIF-2 α protein levels. LNCaP-Pro5 cells were exposed to increasing concentrations of bortezomib (BZ) or NPI-0052 (NPI) for 12 h under normoxic or hypoxic conditions and HIF-1 α was measured by immunoblotting. Actin served as a loading control. **B**, PIs block HIF-1 α transcriptional activity. LNCaP-Pro5 cells were treated as above for 8 h under normoxic or hypoxic conditions. HIF-1 α transcriptional activities were measured using an HRE-driven firefly luciferase expression construct and a renilla luciferase construct as an internal normalization control. Columns, mean; bars, SE; *, $P < 0.001$, compared with controls. **C**, PIs inhibit VEGF expression. LNCaP-Pro5 cells were treated as above for 12 or 24 h under normoxic or hypoxic conditions. VEGF expression was measured by VEGF ELISA (R&D System) in conditioned medium. Columns, mean; bars, SE; *, $P < 0.001$, compared with control (ctrl). **D**, knockdown of HIF-1 α inhibits VEGF expression. siRNA-mediated knockdown of HIF-1 α was carried out as described in Materials and Methods, and VEGF expression was measured by VEGF ELISA (R&D System). Columns, mean; bars, SE; *, $P < 0.001$, compared with control. In parallel, HIF-1 α expression was examined to confirm the silencing efficiency and actin served as a loading control. NS, nonspecific silencing control.

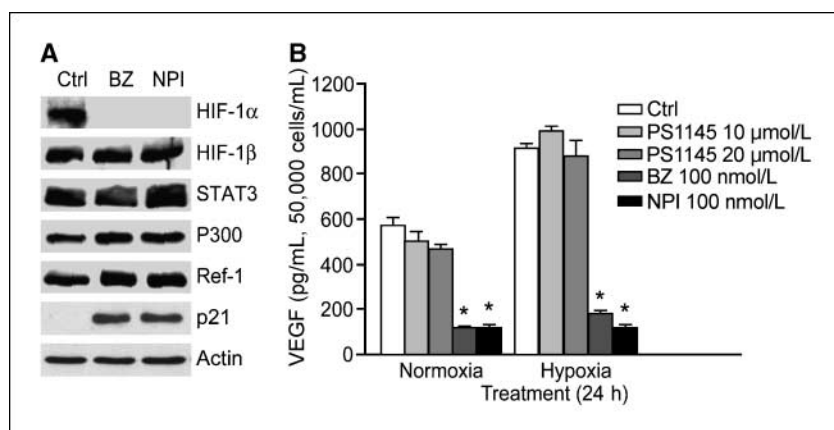


Figure 2. Effects of PIs on other candidate VEGF promoter regulators. *A*, LNCaP-Pro5 cells were exposed to 100 nmol/L bortezomib or 100 nmol/L NPI-0052 for 12 h under hypoxic conditions. Total lysates were probed for expression of HIF-1 α , HIF-1 β , STAT3, p300, Ref-1, or p21^{WAF1} by immunoblotting and actin served as a loading control. *B*, effects of PS-1145 on VEGF expression. LNCaP-Pro5 cells were exposed to 10 or 20 μ mol/L PS-1145, 100 nmol/L bortezomib, or 100 nmol/L NPI-0052 for 24 h under normoxic or hypoxic conditions. VEGF levels were measured by ELISA (R&D System) in conditioned medium. Columns, mean; bars, SE; *, $P < 0.001$, compared with control.

Quantikine ELISA kits (R&D Systems, Inc.). The results were expressed as concentrations of VEGF (pg/mL) per 5×10^4 cells per well. At these time points the drugs did not produce significant toxicity in LNCaP-Pro5 cells.

Luciferase reporter assays. To examine the transcriptional activity of HIF-1 α , LNCaP-Pro5 cells (5×10^4 cells per well) were cotransfected with plasmids encoding a firefly luciferase reporter driven by a promoter containing an HRE and renilla luciferase under the control of an autologous promoter (pRL-CMV; internal control for transfection efficiency) using TransFast (Promega Co.) following the manufacturer's instructions. Luciferase activity was measured using the Dual-luciferase assay system (Promega Co.). Firefly luciferase activity was normalized by renilla luciferase activity and the indicated promoter activities were expressed as the average ratios (\pm SE) from three independent experiments.

Small interfering RNA-mediated silencing of HIF-1 α and eIF2 α . Small interfering RNA (siRNA)-mediated silencing of HIF-1 α and eIF2 α (Dharmacon RNA Technologies) were performed as previously described (16). After silencing, cells were incubated as indicated, VEGF expression was measured by ELISA, and HIF-1 α expression was examined by immunoblotting. The efficiency of gene silencing was verified in each experiment by immunoblotting.

Quantitative real-time-PCR. Total cellular mRNA was isolated using an RNeasy kit (Qiagen) according to the manufacturer's instructions. One microgram of total mRNA was reverse transcribed using SuperArray First-Strand cDNA kit (Superarray Bioscience Co.) and qPCR for HIF-1 α and glyceraldehyde-3-phosphate dehydrogenase (GAPDH; SuperArray Bioscience Co.) were performed in triplicate using a Bio-Rad iCycler real-time PCR system (Bio-Rad Laboratories, Inc.). The amplification protocol consisted of one cycle at 95°C for 3 min, followed by 40 cycles at 95°C for 30 s, 58°C for 30 s, then 72°C for 30 s. The melt-curve protocol, performed at the end of the amplification, consisted of 80 cycles beginning at 55°C for 10 s, and then the temperature was increased by 0.5°C per cycle. A standard curve for each target gene was generated to determine the linear range and amplification efficiency. PCR efficiency of >80% was considered sufficient. The threshold cycle for each sample was fitted to the standard curve to calculate the expression level of the target gene relative to the input mRNA. The resulting data were analyzed with the iCycler iQ Real-time Detection System software and expressed as the mean of ratios (relative expression to control) \pm SE, and GAPDH served as internal loading control.

Polysome profile analysis. Polysome fractionation was performed as previously described (17). Briefly, cells were lysed with polysome lysis buffer [60 mmol/L NaCl, 15 mmol/L Tris-HCl (pH 7.5), 15 mmol/L MgCl₂, 0.5% Triton X-100, 100 μ g/mL cycloheximide, and 1 mmol/L DTT] on ice for 10 min. After centrifugation, supernatants were layered onto 10 mL, 10% to 50% sucrose gradients composed of polysome extraction buffer [60 mmol/L NaCl, 15 mmol/L Tris-HCl (pH 7.5), 15 mmol/L MgCl₂, 100 μ g/mL cycloheximide, and 1 mg/mL heparin]. The gradients were centrifuged at 36,000 rpm for 2 h and 15 min at 4°C in a SW41 rotor (Beckman L8-70M Ultracentrifuge). Gradients were then collected as 0.5 mL fractions by pumping 60% sucrose into the bottom of the gradients and collecting them from the

top using an ISCO fraction collection system (Density Gradient Fractionation System; TELEDYNE, ISCO, Inc.) with concomitant measurement of the absorbance at 254 nm (UA-6; UV-VIS Detector; BRABDEL). Total mRNA from each fraction was extracted using RNeasy kits (Qiagen) and One-step reverse transcription-PCR (RT-PCR) was performed in triplicate using the AgPath-ID One-Step RT-PCR kit (Ambion, Inc.) using primer pairs for HIF-1 α and cyclophilin A (Applied Biosystems). The expression of each target gene was quantified using the StepOne Real-time PCR systems (Applied Biosystems).

Quantification of protein synthesis by [¹⁴C]-Leucine incorporation. Equal numbers of cells were plated in 6-well plates and were incubated with 100 nmol/L bortezomib, 100 nmol/L NPI-0052, 40 μ mol/L cycloheximide, or 10 μ mol/L thapsigargin for 4 h under normoxic conditions. At the end of the experiments, no significant differences in viable cell numbers were observed between untreated and treated samples. Cells were then *trans*-labeled with leucine-free medium (MP Biomedicals) containing [¹⁴C]-Leucine (2 μ Ci/mL, GE Healthcare Bio-Sciences Corp.) for 2 h at 37°C under normoxic conditions. Excess unincorporated [¹⁴C]-Leucine was removed by washing cells with ice-cold PBS. Cells were collected and lysed as previously described. Equal volumes of cellular protein (~20 μ L) from each sample were precipitated by ice cold trichloroacetic acid (10%, w/v) at 4°C for 30 min. Precipitated proteins were then dissolved in 0.1 mol/L KOH and transferred to vials for scintillation counting.

Data analysis. Experiments presented in the figures are derived from or are representative of at least three independent repetitions. Statistical analyses were performed using GraphPad3.05 statistical software (GraphPad Software) using the Student's *t* test, or one-way ANOVA where appropriate (*P* value of <0.05 was considered statistically significant).

Results

Bortezomib and NPI-0052 down-regulate HIF-1 α , HIF-2 α , and VEGF expression. Bortezomib and NPI-0052 inhibit angiogenesis but the molecular mechanisms involved remain unclear (4, 5, 9). HIF-1 α is considered one of the most important proangiogenic transcription factors, and its expression is tightly regulated by the ubiquitin/proteasome degradation pathway (10). We therefore assessed the effects of PIs on HIF-1 α protein accumulation and its transcriptional activity in LNCaP-Pro5 cells. HIF-1 α was almost undetectable under normoxic conditions but was strongly up-regulated by exposure to hypoxia or CoCl₂ (Fig. 1A). Paradoxically, both PIs caused concentration-dependent down-regulation of HIF-1 α protein (Fig. 1A). Both PIs also down-regulated HIF-2 α (Fig. 1A), which is regulated by the proteasome in a similar manner (18). These effects were associated with reduced HIF-1 transcriptional activity (Fig. 1B) and VEGF expression (Fig. 1C). The effects of the PIs were very similar to those caused by HIF-1 α silencing (Fig. 1D).

The VEGF promoter contains several distinct *cis*-acting elements, including the HIF-1 binding sites (HRE) as well as binding sites for signal transducer and activator of transcription 3 (STAT3), activating protein-1, AP-2, NF κ B, and SP-1 (11, 19). We therefore examined the effects of the PIs on several other VEGF regulators in LNCaP-Pro5 cells. We focused on HIF-1 β /ARNT, STAT3, P300, and Ref-1/APE (Redox effector factor-1/apurinic/aprimidinic endonuclease) because these factors form a hypoxia-inducible transcriptional complex with HIF-1 α on the HRE region of VEGF promoter (11, 19, 20). Strikingly, none of these molecules was down-regulated by PIs (Fig. 2A). We also examined the potential role of NF κ B in the PI-mediated suppression of VEGF expression because PIs inhibit NF κ B activity via stabilization of I κ B α . The IKK inhibitor, PS-1145, had no effect on VEGF expression (Fig. 2B), although NF κ B activity was inhibited at these doses as measured by NF κ B electrophoretic mobility shift assay (21).

Biphasic effects of PIs on the stability of HIF-1 α . We next examined the effects of PIs on HIF-1 α stability by immunoblotting

using cellular extracts prepared from cells incubated with the protein translation inhibitor cycloheximide. LNCaP-Pro5 cells were preincubated with CoCl₂ for 16 hours to stimulate HIF-1 α accumulation and then exposed to PIs with or without CHX (Table 1; Fig. 3). Levels of HIF-1 α were detectably lower in CHX-exposed cells compared with controls at 30 minutes and were almost undetectable by 2 hours. In cells exposed to CHX plus PIs, levels of HIF-1 α were ~60% higher than the levels observed in cells exposed to CHX alone at 30 minutes, although HIF-1 α levels were significantly reduced by 2 hours. In cells exposed to PIs alone, HIF-1 α accumulation was observed at 30 minutes (~50% induction compared with control), but HIF-1 α protein levels returned to control levels by 1 hour and then decreased. PIs down-regulated HIF-1 α so rapidly that there was almost no detectable HIF-1 α in cells exposed to the PIs with or without CHX by 4 hours. Based on these observations, we conclude that PIs have biphasic effects on HIF-1 α , causing an early accumulation of HIF-1 α followed by profound down-regulation of protein expression. Importantly, both PIs cause sustained proteasome inhibition in the

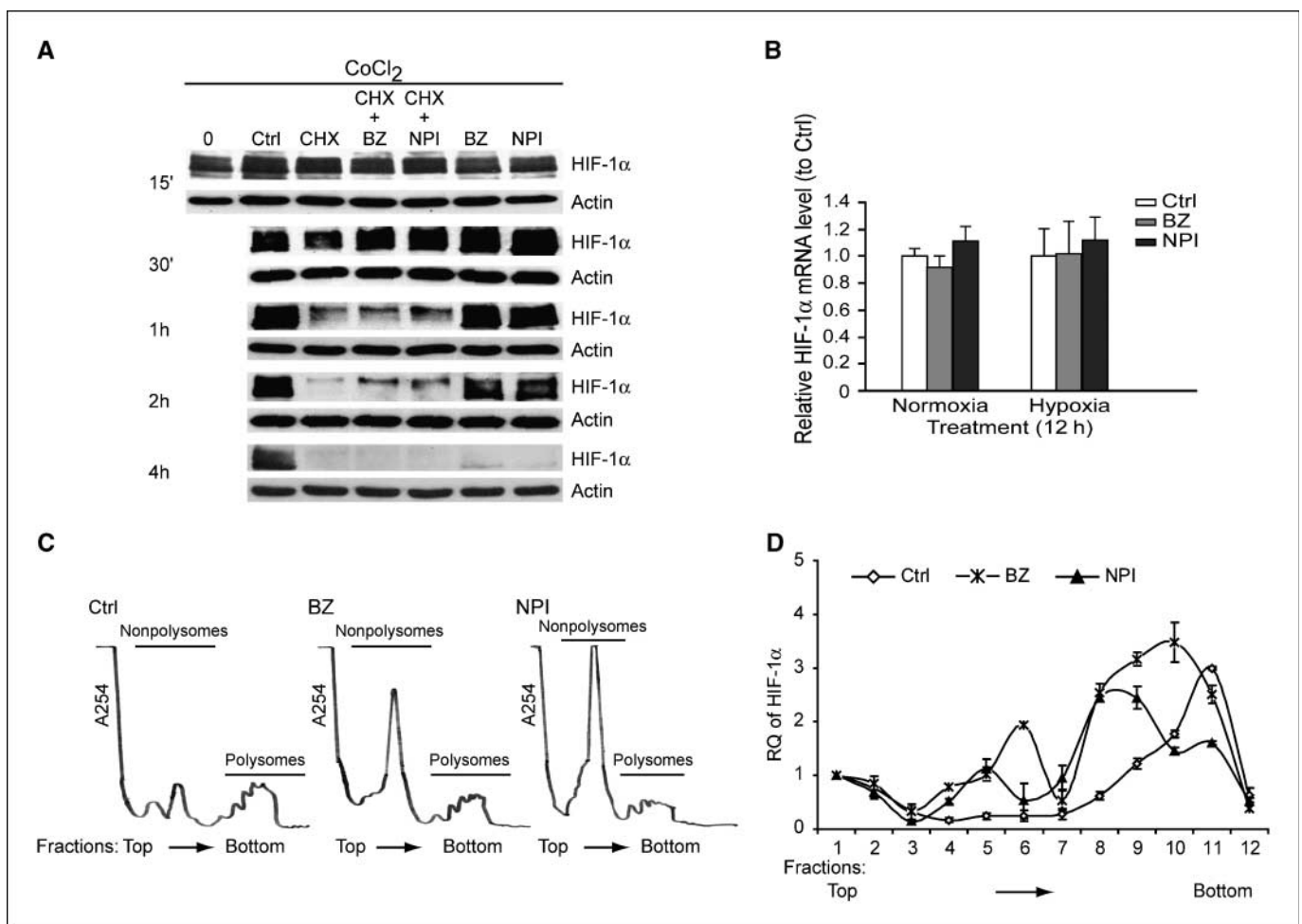


Figure 3. Effects of PIs on HIF-1 α protein stability and HIF-1 α mRNA translation. *A*, biphasic effects of PIs on HIF-1 α stability. LNCaP-Pro5 cells were preincubated with 50 μ M CoCl₂ for 16 h, then exposed to 100 nmol/L bortezomib or 100 nmol/L NPI-0052 with or without 20 μ M CHX for the time indicated in the presence of CoCl₂. Total lysates were probed for HIF-1 α expression by immunoblotting. *B*, PIs have no effect on total HIF-1 α mRNA. LNCaP-Pro5 cells were exposed to 100 nmol/L bortezomib or 100 nmol/L NPI-0052 for 12 h under normoxic or hypoxic conditions. Real-time RT-PCR for HIF-1 α mRNA was performed using the Bio-Rad iCycler. Columns, mean; bars, SE. *C*, PIs induce polysome dissociation. Representative polysome profiles isolated from total cellular lysates fractionated by a continuous sucrose gradient. LNCaP-Pro5 cells were exposed to 100 nmol/L bortezomib or 100 nmol/L NPI-0052 for 4 h. The positions of the polysomes and nonpolysomes (monosomes and mRNPs) are indicated. Note the accumulation of nonpolysomes in the treated cells is indicative of decreased protein translation. *D*, PIs inhibit HIF-1 α translation efficiency. Real-time RT-PCR analysis (RQ) of HIF-1 α mRNA levels in each fraction was performed and the relative mRNA level of the first fraction was arbitrarily set at the value of 1. That HIF-1 α mRNA shifted to lighter fractions in the treated cells is indicative of its translation being repressed. Points, mean; bars, SD.

Table 1. Densitometric quantification of the results shown in Fig. 3A

	15 min	30 min	1 h	2 h	4 h
Ctrl	1	1	1	1	1
CHX	0.85 ± 0.05	0.44 ± 0.11	0.37 ± 0.09	0.14 ± 0.08	0.11 ± 0.04
CHX+BZ	0.81 ± 0.04	0.73 ± 0.25	0.16 ± 0.01	0.17 ± 0.01	0.07 ± 0.02
CHX+NPI	0.78 ± 0.11	0.67 ± 0.28	0.28 ± 0.11	0.20 ± 0.04	0.11 ± 0.01
BZ	0.91 ± 0.08	1.39 ± 0.21	0.93 ± 0.18	0.70 ± 0.19	0.11 ± 0.02
NPI	0.95 ± 0.05	1.76 ± 0.3	0.91 ± 0.12	0.77 ± 0.21	0.10 ± 0.03

NOTE: HIF-1 α /actin levels from untreated cells were arbitrarily set at the value of 1. HIF-1 α signals after normalization to actin levels were expressed as relative densitometry units of the mean of the three repetitions. Data shown are mean \pm SE.

same cells (>24 hours) and other labile proteins do in fact accumulate in the cells at 4 hours and later (Fig. 2A; refs. 6, 16).

Effects of PIs on polysome profiles and HIF-1 α translation efficiency. PIs had no effects on HIF-1 α total mRNA levels (Fig. 3B), which excluded the possibility that PIs inhibit HIF-1 α transcription. Considering that short-lived proteins are particularly sensitive to translational regulation, we performed polysome profiling analysis to directly determine whether or not PIs depress HIF-1 α translation. The results revealed that PIs and thapsigargin (which inhibits the sarcoplasmic/endoplasmic Ca²⁺-ATPase to induce ER stress) induced substantial polysome dissociation and accumulation of monosomes and messenger ribonucleoprotein (mRNP) at 4 hours (Fig. 3C). Longer periods of drug exposure triggered almost complete polysome dissociation (data not shown). We next quantified the relative expression of HIF-1 α and cyclophilin A (internal control) in each fraction using real-time RT-PCR. In untreated cells, the HIF-1 α mRNA peak coincided with heavy polysome fractions, whereas PIs induce the HIF-1 α mRNA to shift to

the lighter fractions, confirming that they disrupt HIF-1 α translation (Fig. 3D). The normally well-translated cyclophilin A mRNA was modestly affected, suggesting that the effects were somewhat selective for HIF-1 α mRNA (data not shown).

Effects of PIs on the unfolded protein response and eIF2 α -dependent protein translation. Recent studies have shown that PIs induce ER stress in cancer cells (7, 8). Cells have evolved the unfolded protein response (UPR) to alleviate ER stress or to induce apoptosis if the stress is excessive. Protein kinase R-like ER kinase (PERK) plays an important role in the UPR by phosphorylating eIF2 α and down-regulating global protein synthesis (22, 23). Bortezomib, NPI-0052, and thapsigargin all induced phosphorylation of PERK and eIF2 α in LNCaP-Pro5 cells (Fig. 4A and B). Hypoxia itself slightly induced eIF2 α phosphorylation, consistent with other studies implicating PERK/eIF2 α in the adaptive response to hypoxia (24, 25). The effects of PIs— or thapsigargin—were associated with inhibition of global protein synthesis as measured by [³H]Leucine incorporation (Fig. 4C), and the inhibitory effects of PIs on protein

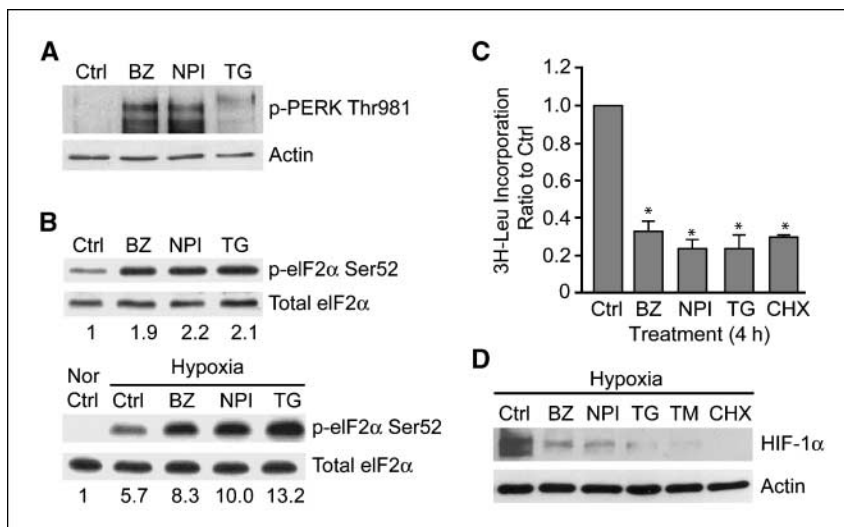


Figure 4. Effects of PIs on the unfolded protein response. **A**, PIs induce PERK phosphorylation. LNCaP-Pro5 cells were exposed to 100 nmol/L bortezomib, 100 nmol/L NPI-0052, or 10 μ mol/L thapsigargin for 4 h and phosphorylated PERK and actin levels were measured by immunoblotting. **B**, PIs induce eIF2 α phosphorylation. LNCaP-Pro5 cells were treated as above under normoxic (*nor*) and hypoxic conditions and phosphorylated and total eIF2 α levels were measured by immunoblotting. The numbers located below each lane correspond to the quantification of the phosphorylated eIF2 α signals by densitometry adjusted to the total eIF2 α protein levels. The phosphorylation of eIF2 α in the untreated group is arbitrarily set at the value of 1. **C**, PIs attenuate general protein synthesis. LNCaP-Pro5 cells were exposed to 100 nmol/L bortezomib, 100 nmol/L NPI-0052, 10 μ mol/L thapsigargin, or 40 μ mol/L cycloheximide for 4 h under normoxic conditions, and protein synthesis was measured by [³H]Leucine incorporation. **Columns**, mean; **bars**, SE, *, $P < 0.001$. **D**, thapsigargin, tunicamycin, and cycloheximide down-regulated HIF-1 α protein levels. LNCaP-Pro5 cells were incubated with 100 nmol/L bortezomib, 100 nmol/L NPI-0052, 10 μ mol/L thapsigargin, 5 μ g/mL tunicamycin, or 40 μ mol/L cycloheximide for 12 h under hypoxic conditions, and HIF-1 α levels were determined by immunoblotting.

synthesis lasted at least 12 hours (data not shown). These data are consistent with the observation that PIs induced polysome dissociation (Fig. 3C). Finally, thapsigargin and another classic ER stress inducer tunicamycin (which inhibits N-linked protein glycosylation) also induced eIF2 α phosphorylation, attenuated protein synthesis, and down-regulated HIF-1 α protein expression (Fig. 4D).

Direct role of eIF2 α phosphorylation in HIF-1 α down-regulation. To determine whether down-regulation of HIF-1 α was phospho-eIF2 α dependent, we first examined the levels of HIF-1 α in LNCaP-Pro5 cells transfected with siRNA specific for eIF2 α or an off-target control construct. PIs induced the accumulation of HIF-1 α in cells depleted eIF2 α , and similar effects were observed in cells exposed to thapsigargin (Fig. 5A). Knockdown of eIF2 α attenuated basal protein synthesis (~35% reduction compared with the off-target control-transfected cells) and partially reversed the effects of PIs on protein translation repression (~60% rescue compared with the off-target control-transfected cells in treated groups; Supplementary Fig. S1). We next compared the effects of

PIs on HIF-1 α in MEF cells expressing wild-type (eIF2 α ^{51SS}) or a phosphorylation-deficient knock-in mutant form of eIF2 α (eIF2 α ^{51AA}). PIs induced phosphorylation of eIF2 α and translational repression in wild-type MEFs but not in the mutant MEFs. Consistent with the results obtained with LNCaP-Pro5 cells, PIs induced strong HIF-1 α accumulation in the mutant MEFs, whereas only have modest effects on HIF-1 α accumulation in the wild-type MEFs (Fig. 5B and C). Thus, PI-induced down-regulation of HIF-1 α is largely eIF2 α phosphorylation dependent.

Cell line-dependent effects of PIs on eIF2 α phosphorylation and HIF-1 α accumulation. PIs induce phosphorylation of eIF2 α in some cancer cell lines but not in others (26–28). Therefore, we characterized the effects of PIs on eIF2 α phosphorylation and HIF-1 α protein levels in three additional genitourinary cancer cell lines (Fig. 6). In PC3 prostate cancer cells, both PIs induced eIF2 α phosphorylation and global translation repression, and these effects were associated with HIF-1 α down-regulation. In contrast, both drugs failed to induce phosphorylation of eIF2 α or inhibit protein synthesis in DU145 or 253JB-V cells, and they actually promoted the accumulation of HIF-1 α in both cell lines. Both PIs inhibited the 20S proteasome and caused accumulation of p21^{WAF1} in all four cell lines (data not shown; Fig. 2A), demonstrating that the observed differences were not caused by differential drug-target interactions. Therefore, the effects of PIs are heterogeneous, and down-regulation of HIF-1 α only occurs in cells that display PIs induced phosphorylation of eIF2 α and protein translation repression.

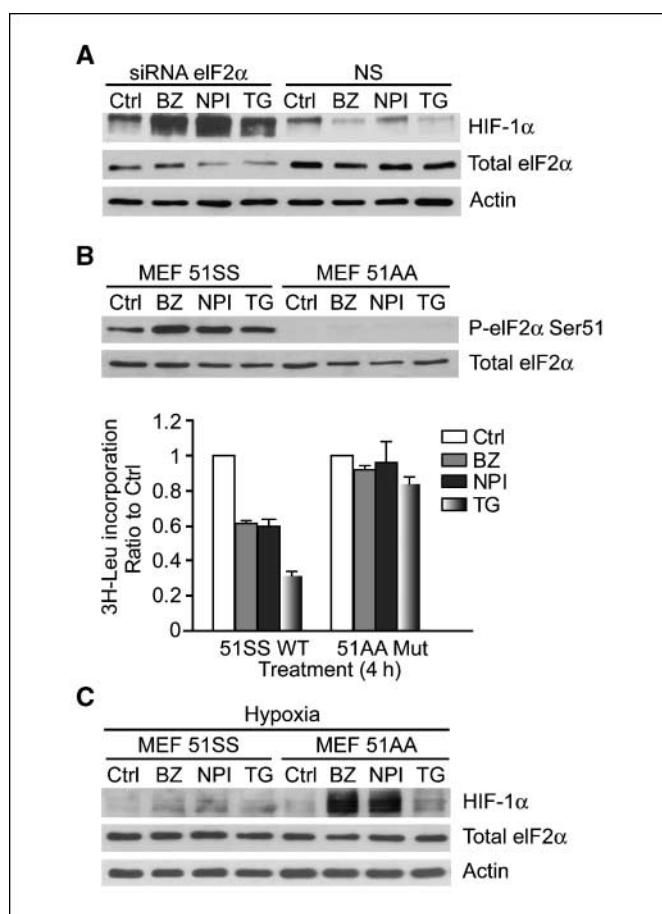


Figure 5. Role of eIF2 α in the effects of PIs on HIF-1 α expression and protein synthesis. **A**, knockdown of eIF2 α rescued HIF-1 α expression. LNCaP-Pro5 cells were transfected with a siRNA construct specific for eIF2 α or a nontargeted control siRNA. Transfected cells were incubated with 100 nmol/L bortezomib, 10 nmol/L NPI-0052, or 5 μ mol/L thapsigargin for 8 h under hypoxic conditions. Levels of HIF-1 α and eIF2 α were examined by immunoblotting and actin served as a loading control. **B**, effects of PIs on eIF2 α and protein translation in MEFs. MEFs were incubated with 100 nmol/L bortezomib, 100 nmol/L NPI-0052, or 10 μ mol/L thapsigargin for 4 h. Phosphorylated eIF2 α (Ser51) and total eIF2 α levels were measured by immunoblotting. Protein synthesis was measured by [3 H]Leucine incorporation. **Columns**, mean; **bars**, SE. **C**, effects of PIs on HIF-1 α in MEFs. MEFs were treated as above for 12 h under hypoxic conditions. Levels of HIF-1 α and total eIF2 α were measured by immunoblotting.

Discussion

Proteasome inhibition is an effective therapeutic strategy for certain cancers, and it also seems to underlie the tissue damage that occurs in neurodegenerative diseases (1, 2, 29). We previously showed that the antitumor effects of bortezomib are associated with suppression of VEGF expression (9). The effects of PIs on VEGF expression are paradoxical given the well-established role VHL/proteasome-mediated degradation plays in the control of HIF-1 α protein expression. Here, we report that PIs induce an unexpected down-regulation of HIF-1 α at translational level via a PERK/eIF2 α -mediated mechanism. Several other antitumor agents, including gefitinib, cetuximab, nelfinavir, and rapamycin, also suppress HIF-1 α expression by blocking its translation. However, these effects involve blockade of the phosphatidylinositol-3-kinase (PI3K)/AKT/glycogen synthesis kinase 3 β /mammalian target of rapamycin (mTOR) pathway (11, 30–32). The PI3K/AKT/mTOR signaling pathway profoundly affects 7-methyl guanosine cap-dependent mRNA translation through phosphorylation of downstream targets such as 4E-BP and S6K and inactivation of the eIF4F translation complex rather than inducing eIF2 α phosphorylation (33). Therefore, it is possible that PIs could be combined with these other agents to produce even stronger inhibition of HIF-1 α -dependent angiogenesis.

We showed here that two cell lines displayed efficient PI-mediated eIF2 α phosphorylation and down-regulation of HIF-1 α (LNCaP-Pro5 and PC3) and two did not (DU145 and 253 JB-V). The basal levels of eIF2 α phosphorylation seemed to correlate with these differences as DU145 and 253 JB-V cells contained high basal phosphorylated eIF2 α and LNCaP-Pro5 and PC3 cells did not. However, there were no measurable differences in global translation rates among the cell lines as measured by [3 H]Leucine incorporation (Supplementary Fig. S2), indicating that basal eIF2 α phosphorylation observed in DU145 and 253JB-V did not activate the protein synthesis checkpoint. We are actively seeking mechanistic explanation(s) for

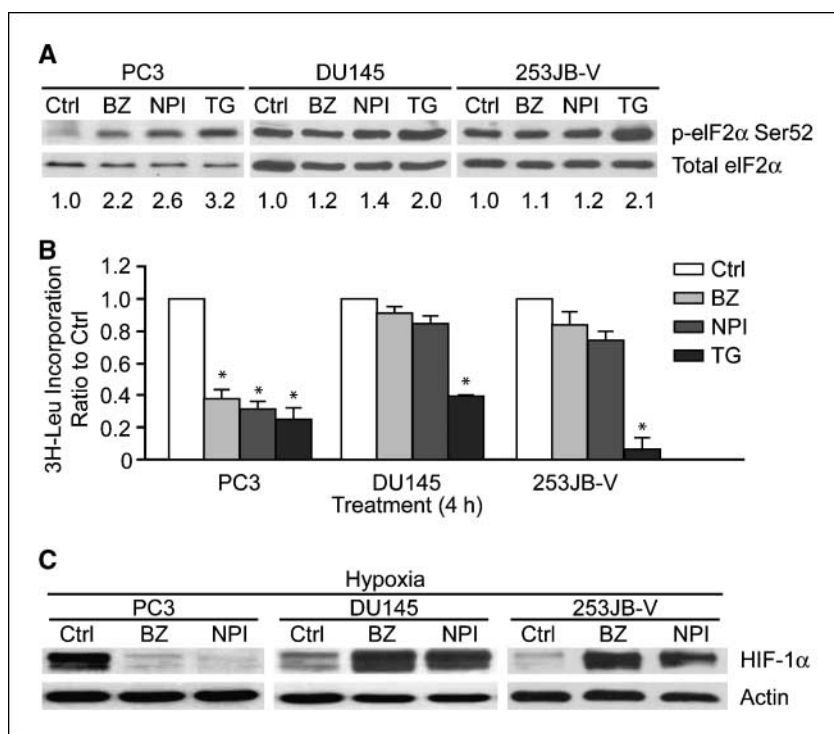


Figure 6. Differential effects of PIs on UPR and HIF-1 α protein levels in different cancer cells. **A**, differential effects of PIs on eIF2 α phosphorylation. PC3, DU145, and 253JB-V cells were incubated with 100 nmol/L bortezomib, 100 nmol/L NPI-0052, or 10 μ mol/L thapsigargin for 4 h. Phosphorylated eIF2 α (Ser52) and total eIF2 α levels were measured by immunoblotting. The numbers located below each lane corresponded to the levels of phospho-eIF2 α , which were determined by densitometry analysis and adjusted to total eIF2 α protein levels. The phosphorylation of eIF2 α in the untreated group was arbitrarily set at the value of 1. **B**, differential effects of PIs on protein synthesis. PC3, DU145, and 253JB-V cells were treated as above for 4 h and protein synthesis was measured by [3 H]Leucine incorporation. Columns, mean; bars, SE; *, $P < 0.001$, compared with control. **C**, differential effects of PIs on HIF-1 α . PC3, DU145, and 253JB-V cells were incubated with 100 nmol/L bortezomib or 100 nmol/L NPI-0052 for 12 h under hypoxic conditions and HIF-1 α levels were measured by immunoblotting.

the observed heterogeneity that eIF2 α is phosphorylated at baseline in some tumor cell lines but not in others.

The proteasome contains three catalytic sites in its inner β -rings (1, 2, 4). We knocked down one (β 5) or all three (β 1, β 2, and β 5) of the active sites of the proteasome using siRNA and measured the effects on protein translation and HIF-1 α protein level. Partial knockdown of proteasome active site(s) attenuated protein translation, but the effects were much less dramatic than those obtained with the chemical inhibitors and caused no obvious HIF-1 α down-regulation (Supplementary Fig. S3). Therefore, we speculate that quantitative differences between the effects of the PIs and proteasome subunits knockdown on translation inhibition and downstream cellular stress responses probably account for the differential effects observed.

The selective effects of PIs on HIF-1 α expression also raise an additional question. Global translational repression would be expected to affect all short-lived proteins, yet p53 and p21 accumulate in LNCaP-Pro5 cells exposed to PIs (Fig. 2A; ref. 34). Furthermore, previous studies reported that phospho-eIF2 α -mediated translational repression were associated with down-regulation of κ B α and cyclin D in MEFs (35, 36), but PIs failed to down-regulate cyclin D in LNCaP-Pro5 cells, whereas thapsigargin did (data not shown). Our explanation for these discrepancies is that the translation of all of these proteins is probably inhibited in a phospho-eIF2 α -dependent manner in cells exposed to PIs, but

what distinguishes the outcome of the protein in question largely depends on whether it is efficiently degraded by a proteasome-independent pathway or not.

Interestingly, other studies have shown that bortezomib has inhibitory effects on HIF-1 α transcriptional activity even when HIF-1 α accumulates (37, 38). Consistent with this conclusion, VEGF expression was blocked by PIs in DU145 and 253JB-V cells (data not shown), although the PIs promoted HIF-1 α accumulation in these two cell lines (Fig. 6). Therefore, PIs might function as HIF-1 α inhibitors regardless of whether they deplete cells of HIF-1 α or not. In future studies, it will be important to determine whether these mechanisms contribute to the antiangiogenic effects of PIs in preclinical models and patient tumors *in vivo*.

Disclosure of Potential Conflicts of Interest

D.J. McConkey: commercial research grant, Millennium Pharmaceuticals and Nereus Pharmaceuticals; honoraria from speakers bureau, Millennium Pharmaceuticals. The other authors disclosed no potential conflicts of interest.

Acknowledgments

Received 10/23/2008; revised 12/12/2008; accepted 12/19/2008; published OnlineFirst 02/24/2009.

The costs of publication of this article were defrayed in part by the payment of page charges. This article must therefore be hereby marked *advertisement* in accordance with 18 U.S.C. Section 1734 solely to indicate this fact.

References

- Adams J. The development of proteasome inhibitors as anticancer drugs. *Cancer Cell* 2004;5:417-21.
- Voorhees PM, Dees EC, O'Neil B, Orlowski RZ. The proteasome as a target for cancer therapy. *Clin Cancer Res* 2003;9:6316-25.
- Richardson PG, Mitsiades C, Hideshima T, Anderson KC. Proteasome inhibition in the treatment of cancer. *Cell Cycle* 2005;4:290-6.
- Adams J, Kauffman M. Development of the proteasome inhibitor Velcade (Bortezomib). *Cancer Invest* 2004;22:304-11.
- Chauhan D, Catley L, Li G, et al. A novel orally active proteasome inhibitor induces apoptosis in multiple myeloma cells with mechanisms distinct from Bortezomib. *Cancer Cell* 2005;8:407-19.
- Ruiz S, Krupnik Y, Keating M, Chandra J, Palladino M, McConkey D. The proteasome inhibitor NPI0052 is a more effective inducer of apoptosis than bortezomib in lymphocytes from patients with chronic lymphocytic leukemia. *Mol Cancer Ther* 2006;5:1836-43.
- McConkey DJ, Zhu K. Mechanisms of proteasome inhibitor action and resistance in cancer. *Drug Resist Updat* 2008;11:164-79.
- Egger L, Madden DT, Rheme C, Rao RV, Bredesen DE. Endoplasmic reticulum stress-induced cell death mediated by the proteasome. *Cell Death Differ* 2007;14:1172-80.
- Williams S, Pettaway C, Song R, Papandreou C.

- Logothetis C, McConkey DJ. Differential effects of the proteasome inhibitor bortezomib on apoptosis and angiogenesis in human prostate tumor xenografts. *Mol Cancer Ther* 2003;2:835-43.
10. Semenza GL. Targeting HIF-1 for cancer therapy. *Nat Rev Cancer* 2003;3:721-32.
11. Ellis LM, Hicklin DJ. VEGF-targeted therapy: mechanisms of anti-tumour activity. *Nat Rev Cancer* 2008;8:579-91.
12. Kaelin WG. Von hippel-lindau disease. *Annu Rev Pathol* 2007;2:145-73.
13. Alqawi O, Moghaddas M, Singh G. Effects of geldanamycin on HIF-1 α mediated angiogenesis and invasion in prostate cancer cells. *Prostate Cancer Prostatic Dis* 2006;9:126-35.
14. Powis G, Kirkpatrick L. Hypoxia inducible factor-1 α as a cancer drug target. *Mol Cancer Ther* 2004;3:647-54.
15. Trastour C, Benizri E, Ettore F, et al. HIF-1 α and CA IX staining in invasive breast carcinomas: prognosis and treatment outcome. *Int J Cancer* 2007;120:1451-8.
16. Lashinger LM, Zhu K, Williams SA, Shrader M, Dinney CP, McConkey DJ. Bortezomib abolishes tumor necrosis factor-related apoptosis-inducing ligand resistance via a p21-dependent mechanism in human bladder and prostate cancer cells. *Cancer Res* 2005;65:4902-8.
17. Lu PD, Harding HP, Ron D. Translation reinitiation at alternative open reading frames regulates gene expression in an integrated stress response. *J Cell Biol* 2004;167:27-33.
18. Chen L, Uchida K, Endler A, Shibasaki F. Mammalian tumor suppressor Int6 specifically targets hypoxia inducible factor 2(α) for degradation by hypoxia- and pVHL-independent regulation. *The Journal of biological chemistry* 2007;282:12707-16.
19. Semenza G. Signal transduction to hypoxia-inducible factor 1. *Biochem Pharmacol* 2002;64:993-8.
20. Gray MJ, Zhang J, Ellis LM, et al. HIF-1 α , STAT3, CBP/p300 and Ref-1/APE are components of a transcriptional complex that regulates Src-dependent hypoxia-induced expression of VEGF in pancreatic and prostate carcinomas. *Oncogene* 2005;24:3110-20.
21. Hideshima T, Chauhan D, Richardson P, et al. NF- κ B as a therapeutic target in multiple myeloma. *J Biol Chem* 2002;277:16639-47.
22. Todd DJ, Lee AH, Glimcher LH. The endoplasmic reticulum stress response in immunity and autoimmunity. *Nature reviews* 2008;8:663-74.
23. Ron D, Walter P. Signal integration in the endoplasmic reticulum unfolded protein response. *Nat Rev Mol Cell Biol* 2007;8:519-29.
24. Bi M, Naczki C, Koritzinsky M, et al. ER stress-regulated translation increases tolerance to extreme hypoxia and promotes tumor growth. *EMBO J* 2005;24:3470-81.
25. Koumenis C, Naczki C, Koritzinsky M, et al. Regulation of protein synthesis by hypoxia via activation of the endoplasmic reticulum kinase PERK and phosphorylation of the translation initiation factor eIF2 α . *Mol Cell Biol* 2002;22:7405-16.
26. Nawrocki ST, Carew JS, Dunner K, Jr., et al. Bortezomib inhibits PKR-like endoplasmic reticulum (ER) kinase and induces apoptosis via ER stress in human pancreatic cancer cells. *Cancer Res* 2005;65:11510-9.
27. Jiang HY, Wek RC. Phosphorylation of the α -subunit of the eukaryotic initiation factor-2 (eIF2 α) reduces protein synthesis and enhances apoptosis in response to proteasome inhibition. *J Biol Chem* 2005;280:14189-202.
28. Obeng EA, Carlson LM, Gutman DM, Harrington WJ, Jr., Lee KP, Boise LH. Proteasome inhibitors induce a terminal unfolded protein response in multiple myeloma cells. *Blood* 2006;107:4907-16.
29. Pandey UB, Nie Z, Batlevi Y, et al. HDAC6 rescues neurodegeneration and provides an essential link between autophagy and the UPS. *Nature* 2007;447:859-63.
30. Semenza GL. Development of novel therapeutic strategies that target HIF-1. *Expert Opin Ther Targets* 2006;10:267-80.
31. Land SC, Tee AR. Hypoxia-inducible factor 1 α is regulated by the mammalian target of rapamycin (mTOR) via an mTOR signaling motif. *J Biol Chem* 2007;282:20534-43.
32. Pore N, Jiang Z, Shu HK, Bernhard E, Kao GD, Maity A. Akt1 activation can augment hypoxia-inducible factor-1 α expression by increasing protein translation through a mammalian target of rapamycin-independent pathway. *Mol Cancer Res* 2006;4:471-9.
33. Easton JB, Houghton PJ. mTOR and cancer therapy. *Oncogene* 2006;25:6436-46.
34. Williams SA, McConkey DJ. The proteasome inhibitor bortezomib stabilizes a novel active form of p53 in human LNCaP-Pro5 prostate cancer cells. *Cancer Res* 2003;63:7338-44.
35. Hamanaka RB, Bennett BS, Cullinan SB, Diehl JA. PERK and GCN2 contribute to eIF2 α phosphorylation and cell cycle arrest after activation of the unfolded protein response pathway. *Mol Biol Cell* 2005;16:5493-501.
36. Deng J, Lu PD, Zhang Y, et al. Translational repression mediates activation of nuclear factor κ B by phosphorylated translation initiation factor 2. *Mol Cell Biol* 2004;24:10161-8.
37. Kaluz S, Kaluzova M, Stanbridge EJ. Proteasomal inhibition attenuates transcriptional activity of hypoxia-inducible factor 1 (HIF-1) via specific effect on the HIF-1 α C-terminal activation domain. *Mol Cell Biol* 2006;26:5895-907.
38. Birle DC, Hedley DW. Suppression of the hypoxia-inducible factor-1 response in cervical carcinoma xenografts by proteasome inhibitors. *Cancer Res* 2007;67:1735-43.

Cancer Research

The Journal of Cancer Research (1916–1930) | The American Journal of Cancer (1931–1940)

Control of HIF-1 α Expression by eIF2 α Phosphorylation–Mediated Translational Repression

Keyi Zhu, WaiKin Chan, John Heymach, et al.

Cancer Res 2009;69:1836-1843. Published OnlineFirst February 24, 2009.

Updated version	Access the most recent version of this article at: doi: 10.1158/0008-5472.CAN-08-4103
Supplementary Material	Access the most recent supplemental material at: http://cancerres.aacrjournals.org/content/suppl/2009/02/23/0008-5472.CAN-08-4103.DC1

Cited articles	This article cites 38 articles, 20 of which you can access for free at: http://cancerres.aacrjournals.org/content/69/5/1836.full#ref-list-1
Citing articles	This article has been cited by 2 HighWire-hosted articles. Access the articles at: http://cancerres.aacrjournals.org/content/69/5/1836.full#related-urls

E-mail alerts	Sign up to receive free email-alerts related to this article or journal.
Reprints and Subscriptions	To order reprints of this article or to subscribe to the journal, contact the AACR Publications Department at pubs@aacr.org .
Permissions	To request permission to re-use all or part of this article, use this link http://cancerres.aacrjournals.org/content/69/5/1836 . Click on "Request Permissions" which will take you to the Copyright Clearance Center's (CCC) Rightslink site.